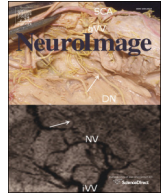




Contents lists available at ScienceDirect

NeuroImage

journal homepage: www.elsevier.com/locate/ynimg

Diffusion properties of major white matter tracts in young, typically developing children

Q1 Ryan T. Johnson^a, Jason D. Yeatman^b, Brian A. Wandell^b, Michael H. Buonocore^c,
4 David G. Amaral^a, Christine W. Nordahl^{a,*}

Q3 ^a M.I.N.D. Institute, Department of Psychiatry and Behavioral Sciences, University of California at Davis, 2825 50th Street, Sacramento, CA 95817, USA

6 ^b Department of Psychology, Jordan Hall, Stanford University, 450 Serra Mall, Stanford, CA 94305, USA

Q5 Q4 ^c Department of Radiology, UC Davis School of Medicine, University of California, Sacramento, CA 95817, USA

ARTICLE INFO

9 Article history:
10 Accepted 14 November 2013
11 Available online xxxx

12 **18** **16** **17** **18** **19** **20** **21** **22**
Keywords:
Children
White matter
Tractography
Development
Sex differences
Laterality

ABSTRACT

Brain development occurs rapidly during the first few years of life involving region-specific changes in both gray 24
matter and white matter. Due to the inherent difficulties in acquiring magnetic resonance imaging data in young 25
children, little is known about the properties of white matter in typically developing toddlers. In the context of an 26
ongoing study of young children with autism spectrum disorder, we collected diffusion-weighted imaging data 27
during natural nocturnal sleep in a sample of young (mean age = 35 months) typically developing male 28
and female (n = 41 and 25, respectively) children. Axial diffusivity, radial diffusivity, mean diffusivity 29
and fractional anisotropy were measured at 99 points along the length of 18 major brain tracts. Influences 30
of hemisphere, age, sex, and handedness were examined. We find that diffusion properties vary signifi- 31
cantly along the length of the majority of tracks. We also identify hemispheric and sex differences in diffu- 32
sion properties in several tracts. Finally, we find the relationship between age and diffusion parameters 33
changes along the tract length illustrating variability in age-related white-matter development at the 34
tract level. 35

© 2013 Elsevier Inc. All rights reserved. 36

Introduction

Early in life the human brain develops quickly. For example, brain 42
volume expands from approximately 25% of adult size at birth to 75% 43
by 2 years of age and 95% by 6 years of age (Knickmeyer et al., 2008; 44
Pfefferbaum et al., 1994). MRI in children and adolescents has revealed 45
rapid growth in both gray matter and white matter but with consider- 46
able regional variability (Giedd et al., 1996; Gilmore et al., 2007, 2012; 47
Huang et al., 2006; Huttenlocher and Dabholkar, 1997; Jernigan et al., 48
1991; Nordahl et al., 2012; Peterson, 2003; Toga et al., 2006). Multiple 49
factors such as age, sex and hemispheric asymmetry likely contribute 50
to this variability in brain growth (Bonekamp et al., 2007; 51
Eluvathingal et al., 2007; Giedd et al., 1997; Lebel and Beaulieu, 2009; 52
Paus et al., 1999; Schmithorst et al., 2008; Trivedi et al., 2009). Account- 53
ing for these factors will produce a more thorough understanding of 54
typical early brain development, which is critical for advancing research 55
in neurodevelopmental disorders (Gabrieli, 2009; Honea et al., 2005; 56
Qju et al., 2008; Thiebaut de Schotten et al., 2011; Yeatman et al., 57
2012a). 58

The inherent difficulties in acquiring magnetic resonance imaging 59
(MRI) data from young children means that relatively little information 60
has been gathered regarding typical brain development prior to 5 years 61
of age. Diffusion-tensor imaging (DTI) allows for detailed exploration of 62
pediatric brain anatomy and has provided important information regard- 63
ing white-matter development. While most major white matter 64
tracts can be identified at birth, examination of tracts in young children 65
has been somewhat lacking with rare exceptions (Dubois et al., 2006; 66
Hermoye et al., 2006; Huang et al., 2006; Qiu et al., 2013; Trivedi et al., 67
2009; Weinstein et al., 2010; Wolff et al., 2012; Yap et al., 2011). 68

White matter tracts consist of thousands of axons entering and 69
exiting at various points to reach specific targets. Thus, using a single 70
diffusion parameter to characterize the entirety of a tract may mask po- 71
tentially valuable information. To account for this variability and pro- 72
vide a detailed characterization of white matter tract structure during 73
early childhood, we used newly available tractography software 74
(Yeatman et al., 2012b) to analyze 18 white matter tracts in typically de- 75
veloping male and female toddlers ranging in age from 26 to 46 months. 76
We quantified diffusion parameters along the length of each tract and 77
identified localized differences while comparing tract properties be- 78
tween hemispheres and in relation to the age and gender of the sub- 79
jects. We found substantial within-tract variability in many tracts as 80
well as location specific sexual dimorphisms and differential effects of 81
age on tract diffusion properties. 82

* Corresponding author at: Department of Psychiatry and Behavioral Sciences,
University of California Davis MIND Institute, Sacramento, CA 95820, USA.
E-mail address: crswu@ucdavis.edu (C.W. Nordahl).

83 Materials and methods

84 Participants

85 Participants were recruited through the M.I.N.D (Medical Investiga-
86 tion of Neurodevelopmental Disorders) Institute of the University of
87 California, Davis (UCD), as part of the Autism Phenome Project. Diffusion
88 imaging data were acquired from typically developing children including
89 41 males and 25 females (Table 1). Participants were recruited as part of
90 a study on autism spectrum disorder, though children with ASD were not
91 included in the present study. Inclusion criteria for the typically develop-
92 ing children included scores within ± 1.5 standard deviations of the
93 mean on all subscales of the Mullen Scales of Early Development. Hand-
94 edness was assessed by means of behavioral examination. Exclusion
95 criteria were physical contraindications to MRI, diagnosis with a perva-
96 sive developmental disorder, specific language impairment or any
97 known developmental, neurological, or behavioral problems. All children
98 were native English speakers. The UCD institutional review board ap-
99 proved this study, and informed consent was obtained from the parent or
100 guardian of each participant.

101 Imaging procedures

102 MRI scans were acquired during natural nocturnal sleep at the UC
103 Davis Imaging Research Center using a 3T Siemens Trio whole-body
104 MRI system (Siemens Healthcare, Inc., Erlangen, Germany) equipped
105 with an 8-channel head coil (Invivo, Inc., Gainesville, FL). The scanner
106 room was decorated to be child-friendly with colorful wall hangings,
107 pillows and stuffed animals. Earplugs and/or headphones were used
108 to attenuate scanner noise and children were closely monitored during
109 scanning. This approach has proven highly successful with a success
110 rate of over 85% (Nordahl et al., 2008).

111 For all participants, images were obtained using a three-dimensional
112 T1-weighted MPRAGE sequence (TR 2170 ms; TE 4.86 ms; matrix
113 256×256 ; 192 slices in the sagittal direction, 1.0 mm isotropic voxels,
114 scan time: 8 m 6 s) and a diffusion-weighted, spin echo, echo planar
115 imaging sequence (“ep2d_diff”, number of slices: 72, slice thickness:
116 1.9 mm, slice gap: 0.0, matrix size: 128×128 , voxel size: 1.9 mm iso-
117 tropic, phase encoding direction: anterior to posterior ($A >> P$), phase
118 partial Fourier: 5/8, TR: 11500, TE: 91, scan time: 6 m 56 s), with effec-
119 tive b-value $700 \text{ mm}^2/\text{s}$, 30 gradient directions, and five $b = 0$ images
120 acquired at equally spaced intervals over the scan time. T2-weighted
121 images were also obtained for clinical evaluation when possible (i.e.
122 when the child remained asleep). All MPRAGE and available T2 scans
123 were reviewed by a pediatric neuroradiologist and screened for signifi-
124 cant, unexpected clinical findings.

125 Images were acquired from October 2007 to June 2011. In August
126 2009, the Siemens 3T Trio MRI system was upgraded to a Trio Total Im-
127 aging Matrix (TIM) MRI System running version VB15A operating sys-
128 tem software. All the VA25A sequences were upgraded and mapped

to their corresponding VB15A sequences with no parameter changes 129
having an effect on image quality or appearance, except for the 130
diffusion-weighted sequence. For this sequence, the spatial resolution, 131
b-value, and diffusion gradient directions were preserved, but param- 132
eters were changed to reduce the geometric distortion of the images, and 133
the impact of the geometric distortion on the image analysis. Specifical- 134
ly, the phase encoding direction was changed from ‘anterior to posteri- 135
or’ ($A >> P$) to ‘posterior to anterior’ ($P >> A$), to eliminate tissue 136
compression in the anterior temporal and frontal lobes, and the iPAT op- 137
tion (GRAPPA) was used with a factor 2 acceleration to permit shorter 138
TE and reduced effective echo spacing for reduced geometric distortion 139
at all voxels. The phase partial Fourier factor was increased from 5/8 to 140
6/8 to partially compensate for the factor 2 reduction in data acquired 141
using GRAPPA. The use of GRAPPA allowed TE to be reduced from 142
91 ms to 81 ms, and echo spacing to be reduced from 0.83 ms to 143
0.69 ms. It also allowed TR to be reduced from 11,500 ms to 8500 ms, 144
and scan time from 6 m 56 s to 5 m 23 s. Although the diffusion gradi- 145
ent parameters (directions and b-value) were not changed, the reduc- 146
tion in geometric distortion caused averaging (over the local tissue to 147
determine each voxel value) to be different in the pre-upgrade versus 148
post-upgrade images. Thus, there are likely to be differences in the 149
diffusion parameters in regions with reduced geometric distortion. To 150
control for these differences, we included MRI system upgrade status 151
(pre-upgrade, post-upgrade) as a nuisance covariate for all statistical 152
analyses involving diffusion parameters. In the current study, 29 scans 153
(10 females, 20 males) were acquired before the scanner upgrade and 154
37 scans were acquired (15 females, 22 males) afterwards (Fisher’s 155
exact test, $p = 0.62$). 156

Image processing and diffusion tensor calculation 157

158 T1-weighted structural image preprocessing follows Nordahl et al. 158
(2011) and included removal of nonbrain tissue using the Oxford Center 159
for Functional MRI of the Brain (FMRIB) brain extraction tool (BET; 160
Smith, 2002) and correction of main field (B_0) inhomogeneities using 161
the nonparametric nonuniform-intensity normalization method (N3; 162
Sled et al., 1998). DTI data were processed using the VISTALab (Stanford 163
Vision and Imaging Science and Technology) diffusion MRI software 164
suite. The raw DTI DICOM images were converted to 4-D NifTI format 165
and volumes and motion artifacts were excluded. DTI images were 166
aligned to the motion-corrected mean of the non-diffusion weighted 167
($b = 0$) images using a rigid body algorithm. DTI images were then 168
resampled to 2-mm isotropic voxels with eddy-current and motion cor- 169
rection using a 7th-order b-spline algorithm based on SPM5. VISTALab 170
image processing software is available as part of the open-source 171
mrDiffusion package available at <http://white.stanford.edu/software/>. 172

173 Diffusion tensors were fitted to the resampled DTI data using a least 173
squares fit and the RESTORE algorithm that also removed outliers from 174
the tensor estimation (Chang et al., 2005). The diffusion tensor model 175
produces measures describing the diffusion characteristics of each 176
voxel. Eigenvalues ($\lambda_1, \lambda_2, \lambda_3$) from the diffusion tensor are used to 177
compute axial diffusivity (λ_1), radial diffusivity ($(\lambda_2 + \lambda_3)/2$), mean dif- 178
fusivity ($(\lambda_1 + \lambda_2 + \lambda_3)/3$) and fractional anisotropy ($\sqrt{(1/2)\sqrt{179$
 $((\lambda_1 - \lambda_2)^2 + (\lambda_2 - \lambda_3)^2 + (\lambda_3 - \lambda_1)^2) / \sqrt{(\lambda_1^2 + \lambda_2^2 + \lambda_3^2)}}$) 180
(Pierpaoli and Basser, 1996). Axial diffusivity (AD) describes diffusion 181
parallel to the principle diffusion direction (i.e. along the long axis of a 182
fascicle of fibers) and has been related to changes in axon integrity such as 183
during axonal degeneration (Kim et al., 2007; Song et al., 2003; Sun 184
et al., 2006; Thomalla et al., 2004). Radial diffusivity (RD) describes diffu- 185
sion perpendicular to the principle diffusion direction and is decreased 186
with reduced axonal myelination or axon tract density (Song et al., 187
2002, 2003; Tyszka et al., 2006; Zhang et al., 2009). Mean diffusivity 188
(MD) and fractional anisotropy (FA) are summative measures that de- 189
scribe average total diffusion and a normalized standard deviation of 190
the three diffusion directions, respectively. 191

Q2 Table 1

t1.2 Description of participants.

t1.3	Continuous descriptors	Mean (SD)	Categorical descriptors	N (%)
t1.4	Age in months	35.28 (4.71)	Left handed	6 (9.09)
t1.5	Mullen’s visual reception t-score	56.23 (11.04)	Right handed	58 (87.88)
t1.6	Mullen’s receptive language t-score	52.92 (7.28)	Undetermined	2 (3.03)
t1.7	Mullen’s expressive language t-score	55.49 (8.73)	Caucasian	51 (77.3)
t1.8	Mullen’s fine-motor t-score	50 (12.68)	Asian	6 (9.1)
t1.9			African-	3 (4.5)
			American	
t1.10			Pacific-Islander	1 (1.5)
t1.11			Other	2 (3.0)
t1.12			Not specified	3 (4.5)

192 Automatic fiber quantification

193 We used Automatic Fiber Quantification (AFQ) software tools to
 194 identify 18 white matter tracts in each participant's brain. AFQ and con-
 195 sists primarily of steps: (1) whole-brain tract tractography, (2) ROI-
 196 based tract segmentation and cleaning and (3) quantification. After
 197 ROI-based segmentation, fiber tracts were cleaned using a statistical
 198 outlier rejection algorithm. First each fiber in a fiber group is sampled
 199 to 99 equidistant nodes. Then the spread of fibers at each node is repre-
 200 sented as a 3 dimensional Gaussian distribution and any fiber that is
 201 more than 5 standard deviation from the core (mean) of the tract is re-
 202 moved. The procedure is repeated until there are no more fiber outliers.
 203 Diffusion properties are then calculated along the trajectory of the fiber
 204 group by interpolating the image value (FA, MD, AD, RD) at each node
 205 along each fiber. Tract profiles of each parameter are then calculated
 206 as a weighted sum of each fiber's value at a given node where a fiber
 207 is weighted based on its Mahalanobis distance from the core or mean lo-
 208 cation of the tract. AFQ tractography yields tracts similar to those seen in
 209 other reports in this participant age range (Fig. 1, Huang et al., 2006;
 210 Trivedi et al., 2009; Wolff et al., 2012). Furthermore, tractography re-
 211 sults generally match the overall shape and anatomical paths seen in
 212 older children and adults (Goodlett et al., 2009; Hermoye et al., 2006;

Huang et al., 2006; Lebel et al., 2012). AFQ is described in greater detail 213
 in Yeatman et al. (2012b). 214

Because AFQ uses strict criterion for tract identification, it did not 215
 identify all 18 tracts in each participant. As might be expected, image 216
 quality was a significant determinant of AFQ's ability to segment and 217
 identify tracts, and there was greater success with scans acquired after 218
 the scanner and sequence update (see Imaging procedures section). De- 219
 tails regarding tract identification rates and their influence on the total 220
 N used in analysis are shown in Table 2. 221

For the most part, tract identification did not differ in the left and 222
 right hemispheres. However, both the cingulum and arcuate fasciculus 223
 had greater probability of identification in the left hemisphere than in 224
 the right (left cingulum 85%, right cingulum 71%, Fisher's exact test 225
 $p < 0.05$; left arcuate fasciculus 87%, right arcuate fasciculus 52%, Fisher's 226
 exact test $p < 0.001$). Difficulty in identifying the right arcuate fas- 227
 ciculus using tractography is a consequence of the right tract 228
 exhibiting higher curvature and greater partial voluming with the super- 229
 ior longitudinal fasciculus compared with the left arcuate fasciculus 230
 (Catani et al., 2007; Lebel and Beaulieu, 2009; Mishra et al., 2010; 231
 Yeatman et al., 2011). Laterality of cingulum diffusion parameters has 232
 been previously reported in adults (Gong et al., 2005a). The significant 233
 asymmetry in all four diffusion parameters for the cingulum likely con- 234
 tributed to the difference in identification rates and is discussed in more 235
 detail below. 236

Tract identification was also not influenced by participant sex with 237
 the exception of the right and left inferior longitudinal fascicles (ILF; 238
 Fisher's exact test, $ps < 0.001$). These tracts were identified less often 239
 in males than in females. Sex differences in diffusion parameters have 240
 been found in the ILF previously (Choi et al., 2010) and in the current 241
 study (see Effects of sex section). If diffusion is lower in males through 242
 much of this tract's bundle, this may lead to a greater chance of exclu- 243
 sion during tractography. 244

Statistical approach 245

For each subject, AD, RD, MD, and FA were calculated at 99 nodes be- 246
 tween the two defining ROIs for each tract. For all differential analysis, 247
 separate three-way mixed-design analyses of co-variance (ANCOVA) 248
 were conducted for the continuous dependent variables (AD, RD, MD, 249
 FA). Hemisphere and nodes were used as repeated measures and 250
 sex as a between-group measure. For hemisphere analysis in the 251
 forceps major and minor nodes 1–49 were compared to nodes 50–99. 252

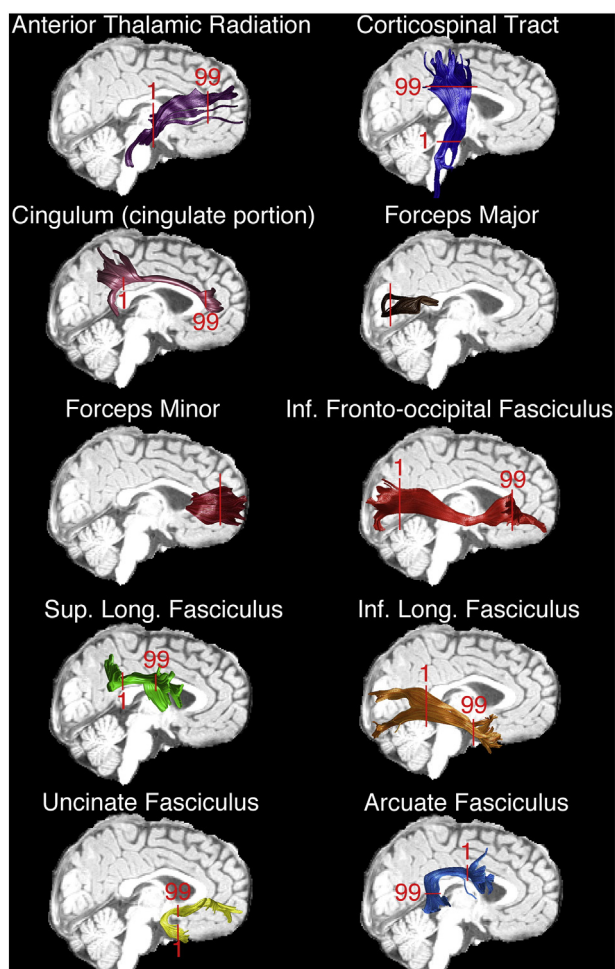


Fig. 1. White-matter tracts examined. AFQ tractography identifies major white matter tracts in children between 26 and 48 months. Single subject results are shown for each of the tracts used in the current analysis. In addition, red markers denoting the start (1) and termination (99) of nodal quantification are overlaid onto each tracts bundle. In the forceps major and minor quantification originated in the left hemisphere and proceeded to the right.

Table 2

Tract identification rates.

Tract name	Preupgrade scans (%)	Postupgrade scans (%)	Total N used in analyses	
Left thalamic radiation	86.67	100.00	63	t2.1
Right thalamic radiation	96.67	100.00	66	t2.2
Left corticospinal	96.67	100.00	66	t2.3
Right corticospinal	96.67	100.00	66	t2.4
Left cingulum	66.67	100.00	57	t2.5
Right cingulum	46.67	91.89	48	t2.6
Forceps major	50.00	100.00	52	t2.7
Forceps minor	100.00	100.00	67	t2.8
Left inferior fronto-occipital	80.00	100.00	61	t2.9
Right inferior fronto-occipital	83.33	100.00	62	t2.10
Left inferior longitudinal	70.00	100.00	58	t2.11
Right inferior longitudinal	66.67	94.59	55	t2.12
Left superior longitudinal	93.33	97.30	64	t2.13
Right superior longitudinal	96.67	100.00	66	t2.14
Left uncinate	93.33	100.00	65	t2.15
Right uncinate	96.67	100.00	66	t2.16
Left arcuate	80.00	91.89	58	t2.17
Right arcuate	56.67	48.65	35	t2.18

Participant's age was included as a continuous covariate while handedness and scanner status were controlled.

Mauchly's test of sphericity (Mauchly, 1940) was used to test for violations of sphericity and the Greenhouse–Geisser correction (Greenhouse and Geisser, 1959) was applied when sphericity was violated. Follow-up one-way ANCOVAs and Bonferroni-corrected pairwise comparisons were used to further investigate significant main-effects and interactions identified in the omnibus tests. Because the repeated measure of nodes was nested within the repeated measure of hemisphere, pairwise comparisons of hemisphere mean differences (averaged across nodes) were considered useful and informative in the absence of significant omnibus hemisphere effects. For correlations between age and diffusion properties, partial correlations controlling for scanner upgrade status were used. For all analyses, results are expressed as mean \pm SEM (standard error of the mean), and a p-value less than 0.05 was considered statistically significant.

Results

Effects of hemisphere

For all tracts except the forceps minor, significant effects of hemisphere were seen for most of the diffusion parameters (Fig. 2, Table 3). When significantly different, mean AD was generally higher in the right hemisphere, with the only exception being in the cingulum. Similarly, mean RD was usually higher in the right hemisphere. Mean MD was also higher in the right hemisphere for several tracts. Mean FA was higher in several left hemisphere tracts. It was higher in the right hemisphere only for the superior longitudinal fasciculus (SLF). Corrected comparisons between hemisphere diffusion parameter means are detailed in Table 3.

In every case in which FA was greater in one hemisphere, AD and/or RD were asymmetric as well. However, in the thalamic radiation and uncinate fasciculus, AD or RD was asymmetric without an asymmetry in FA. Due to the substantial between hemisphere variability indicated by these analyses, subsequent analyses reported below were conducted independently for each hemisphere.

Effects of nodes

For the majority of tracts, diffusion properties varied significantly along the length of the tract (Fig. 2). AD, RD and MD were significantly variable in 8, 6 and 10 tracts respectively. FA was variable in 4 tracts. Only the left inferior fronto-occipital fasciculus (IFOF), left and right inferior longitudinal fasciculi (ILF), and left and right superior longitudinal fasciculi (SLF) exhibited relative homogeneity along their length for all diffusion properties. Statistical comparisons for the effects of nodes on each tract are shown in Table 4.

Effects of sex

Male and female participants exhibited significant differences in the diffusion parameters in 4 tracts. The most prominent sex difference was seen in the left cingulum bundle (Fig. 3). AD in the cingulum was greater in males than in females (main effect of sex: $F(1,98) = 5.71, p < 0.05$). Corrected comparisons revealed that the AD differences were restricted mostly to two bands of nodes along the tract length; one caudal portion of the anterior cingulate and a second larger band adjacent to the posterior cingulate. RD was higher in females than in males (main effect of sex: $F(1,98) = 5.95, p < 0.05$). This was restricted to one large band of nodes near the posterior cingulate. The elevated AD in males and elevated RD in females also resulted in a sex difference in FA (main effect of sex: $F(1,98) = 9.93, p < 0.005$) with FA being higher in males than in females in both a small band at the anterior end of the tract and a larger band at its posterior portion.

Sex differences were also found in the right IFOF (Fig. 4). AD was higher in males (main effect of sex: $F(1,98) = 5.24, p < 0.05$). Although there was a small band of significantly different AD near the anterior portion of the IFOF, the largest band of difference was at the posterior end of the tract. Mean diffusivity was also higher in males in this location (interaction of nodes and sex: $F(1,2.38) = 2.95, p < 0.05$).

Additional sex differences were found in the left ILF and right uncinate fasciculus (Fig. 5). FA was higher in females in the left ILF in two distinct bands towards the anterior end of the tract (main effect of sex: $F(1,98) = 7.17, p < 0.05$). FA was also higher in females in the right uncinate in a band near the temporal end of the tract (interaction of nodes and sex: $F(1,4.47) = 2.69, p < 0.05$).

Two tracts had additional interactions involving participant sex. In the cingulum, the interaction between hemisphere and sex was significant ($F(1,98) = 4.69, p < 0.05$) with females exhibiting less laterality than males (females: left hemisphere 0.41 ± 0.10 , right hemisphere 0.39 ± 0.01 ; males: left hemisphere 0.48 ± 0.01 , right hemisphere 0.041 ± 0.01). In the uncinate, the interaction between sex, hemisphere, and nodes was significant for RD ($F(1,5.49) = 2.97, p < 0.05$) and FA ($F(1,5.3) = 2.58, p < 0.05$). RD is lower in the right uncinate fasciculus compared with the left in the temporal portion of the tract and then becomes higher in the right uncinate compared with the left in females. In males, RD is higher in the right uncinate fasciculus compared with the left and then becomes lower compared with the left as the tract passes into the frontal lobe.

Age as a covariate of interest

We found age to be a significant contributor to variation in 5 tracts: the forceps minor, left IFOF, left SLF, left uncinate fasciculus, and right arcuate fasciculus. For the forceps minor, the left IFOF and the left uncinate fasciculus, age was significant as a main effect. In the left and right arcuate fasciculi, age emerged in a significant interaction with nodes. We chose to examine the correlations between age and diffusion parameters in these tracts.

Examining partial correlations at each node (scanner status and handedness controlled) revealed substantial variation in the correlation between age and diffusion parameters (Fig. 6). In the forceps minor, RD, AD and MD were negatively correlated with age. However, the relationship was particularly strong near where the forceps minor passes through the genu of the corpus callosum. In the left IFOF, FA exhibited a variable but mostly positive relationship with age; the strongest correlations were near the frontal end of the tract. AD in the left SLF was both negatively and positively correlated with age with a strong positive correlation near the frontal termination of the tract. In the left uncinate fasciculus, MD is most strongly correlated with age as the tract begins to leave the temporal lobe and passes near the IFOF. The right arcuate exhibited highly variable correlations with age along the tract length for RD, MD and FA. For each diffusion parameter in the arcuate fasciculus, correlations reversed in sign near the temporo-parietal termination point of the tract.

Participant handedness as a covariate

Evidence for a handedness effect on white-matter diffusion parameters in young children is limited. However, handedness effects have been revealed in adults in some tracts (Gong et al., 2005a). We included handedness as a covariate to control for potential confounding effects without specific hypotheses. Handedness emerged as a significant covariate in seven tracts for various diffusion parameters: FA in the right corticospinal tracts, MD in the left cingulum, FA, AD, MD and RD in the forceps minor, FA in the right IFOF, FA in the right ILF, FA in the right uncinate and RD, MD in the right arcuate. In general, FA tended to be higher and MD lower in right handed subjects compared with left handed subjects.

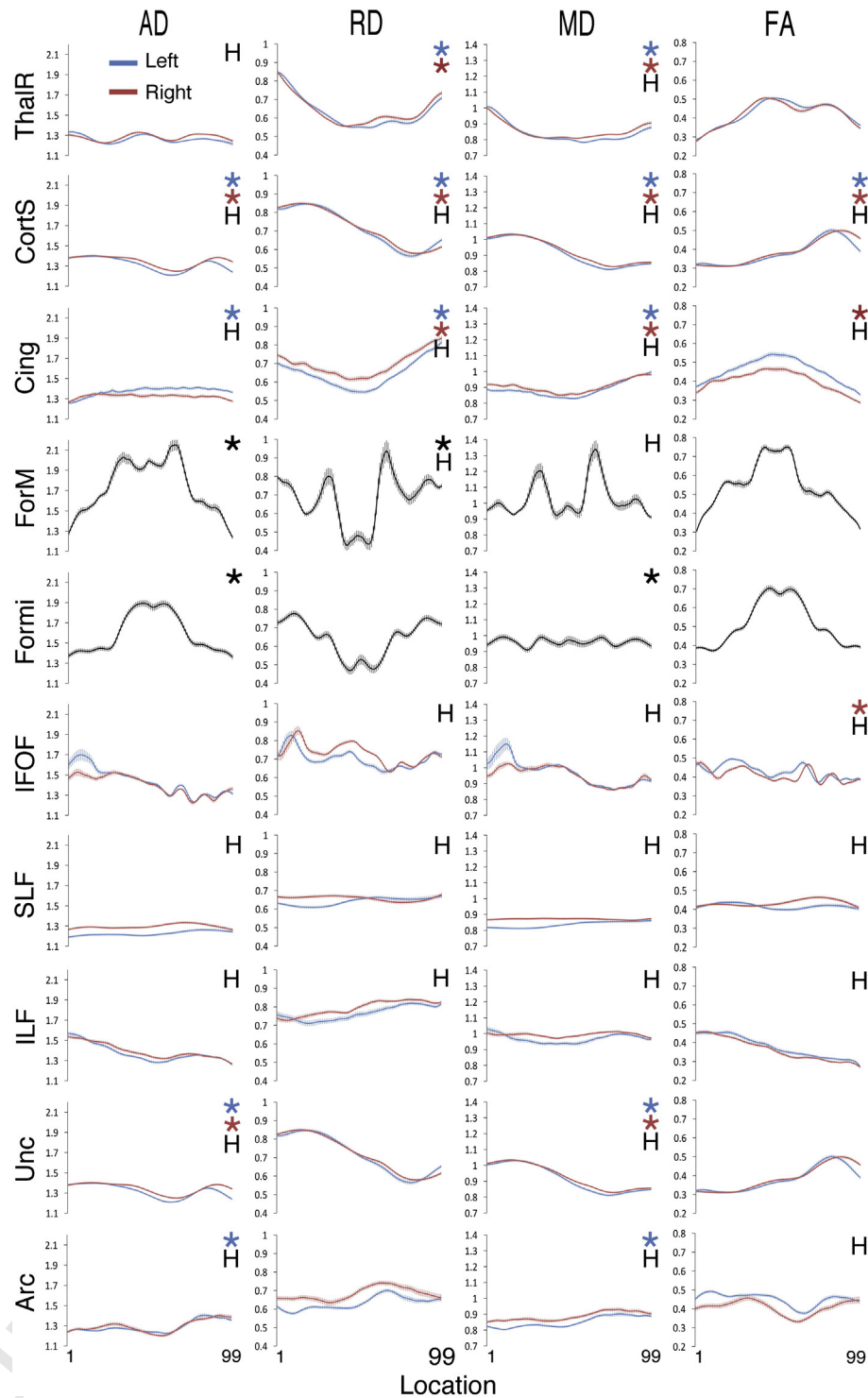


Fig. 2. Diffusion parameters vary along the length of tracts. Average diffusion parameter plots in 18 tracts from typically developing children. Each plot depicts AD, RD, MD or FA between the 1st and 99th nodes of each tract named at left. Tract names are abbreviated as follows: ThalR = thalamic radiations, CortS = corticospinal tracts, Cing = cingulum, ForM = forceps major, Formi = forceps minor, IFOF = inferior fronto-occipital fasciculus, SLF = superior longitudinal fasciculus, ILF = inferior longitudinal fasciculus, Unc = uncinate fasciculus, Arc = arcuate fasciculus. On each plot, "H" denotes a significant difference between the left and right hemispheres and * indicates a significant effect of location for the diffusion parameter plotted.

372 Discussion

373 Differences in the progression of tract diffusion parameters are
 374 thought to reflect differential rates of axonal refinement, packing and
 375 myelination as part of overall white matter maturation (Beaulieu,
 2002; Song et al., 2002, 2005; Takahasi et al., 2000; but see Wheeler-

Kingshott et al., 2009). However, few studies have investigated the variation in diffusion parameters along the length of major fasciculi in relation to hemisphere and sex before the age of 5, a time when the brain is changing rapidly. We found diffusion parameter variability related to sex, hemisphere and age in multiple white matter tracts within a sample of 26–46 month old typically developing young children. In

Table 3
Hemisphere differences in tract diffusion properties.

Tract name	Left hemisphere Mean (95% CI)	Right hemisphere Mean (95% CI)	Pairwise p-value
<i>Thalamic radiation</i>			
AD*	1.26 (1.25–1.27)	1.28 (1.27–1.29)	0.00
RD	0.63 (0.62–0.63)	0.63 (0.62–0.64)	0.20
MD*	0.84 (0.83–0.85)	0.85 (0.84–0.85)	0.01
FA	0.43 (0.42–0.43)	0.43 (0.42–0.44)	0.60
<i>Corticospinal tract</i>			
AD*	1.42 (1.41–1.43)	1.49 (1.47–1.50)	0.00
RD*	0.55 (0.54–0.56)	0.62 (0.60–0.63)	0.00
MD*	0.84 (0.83–0.85)	0.91 (0.90–0.92)	0.00
FA*	0.55 (0.54–0.56)	0.52 (0.51–0.53)	0.00
<i>Cingulum</i>			
AD*	1.38 (1.35–1.40)	1.32 (1.30–1.34)	0.00
RD*	0.64 (0.62–0.65)	0.69 (0.68–0.71)	0.00
MD*	0.88 (0.87–0.90)	0.90 (0.89–0.92)	0.01
FA*	0.46 (0.45–0.47)	0.40 (0.39–0.41)	0.00
<i>Inferior fronto-occipital</i>			
AD	1.41 (1.40–1.43)	1.42 (1.40–1.44)	0.51
RD*	0.70 (0.69–0.71)	0.73 (0.72–0.74)	0.00
MD*	0.94 (0.93–0.95)	0.96 (0.95–0.97)	0.00
FA*	0.43 (0.42–0.44)	0.41 (0.40–0.42)	0.00
<i>Superior longitudinal</i>			
AD*	1.23 (1.21–1.24)	1.30 (1.28–1.32)	0.00
RD*	0.64 (0.63–0.66)	0.66 (0.65–0.67)	0.01
MD*	0.84 (0.82–0.85)	0.87 (0.86–0.89)	0.00
FA*	0.42 (0.40–0.43)	0.43 (0.42–0.44)	0.01
<i>Inferior longitudinal</i>			
AD*	1.37 (1.36–1.39)	1.39 (1.38–1.41)	0.02
RD*	0.75 (0.74–0.76)	0.79 (0.78–0.80)	0.00
MD*	0.96 (0.95–0.97)	0.99 (0.98–1.00)	0.00
FA*	0.39 (0.38–0.39)	0.36 (0.36–0.37)	0.00
<i>Uncinate</i>			
AD*	1.32 (1.30–1.33)	1.35 (1.34–1.36)	0.00
RD	0.71 (0.70–0.72)	0.72 (0.71–0.73)	0.31
MD*	0.91 (0.91–0.92)	0.93 (0.92–0.93)	0.00
FA	0.38 (0.38–0.39)	0.39 (0.38–0.40)	0.05
<i>Arcuate</i>			
AD	1.30 (1.27–1.32)	1.29 (1.27–1.31)	0.40
RD*	0.63 (0.61–0.65)	0.68 (0.66–0.70)	0.00
MD*	0.85 (0.84–0.87)	0.88 (0.87–0.90)	0.00
FA*	0.46 (0.44–0.47)	0.41 (0.39–0.42)	0.00
<i>Forceps major</i>			
AD	1.75 (1.70–1.79)	1.73 (1.68–1.77)	0.08
RD*	0.64 (0.61–0.68)	0.71 (0.66–0.75)	0.04
MD*	1.01 (0.97–1.05)	1.05 (1.00–1.09)	0.04
FA	0.57 (0.55–0.59)	0.52 (0.50–0.54)	0.10
<i>Forceps minor</i>			
AD	1.61 (1.60–1.63)	1.63 (1.61–1.64)	0.74
RD	0.66 (0.64–0.67)	0.65 (0.63–0.66)	0.34
MD	0.96 (0.96–0.99)	0.98 (0.96–0.99)	0.35
FA	0.52 (0.51–0.53)	0.53 (0.52–0.54)	0.32

* Denotes a significant between hemisphere differences with $p < 0.05$.

addition, we found that diffusion parameters vary substantially along the length of a single fiber tract.

Diffusion parameters vary along tract length in young children

Previous reports have measured integrated mean diffusion parameters across the entire tract within the age range reported here (Fletcher et al., 2010; Hermoye et al., 2006; Lebel et al., 2012; Trivedi et al., 2009). However, this is the first report to describe within-tract variability at this age. The variations in diffusion at different sample positions likely reflect a combination of factors including variations in myelination, axonal density, and axonal diameter as well as the influence of tract

curvature, partial voluming effects and the entrance and exit of smaller axonal bundles from the larger tract (Fig. 7). Diffusion properties are affected by biological properties of the axons in a voxel (e.g. myelination, axonal density and axonal diameter) as well as the geometric configuration of the axons (e.g. curvature, directional coherence and crossing fiber tracts). We find that diffusion properties vary substantially along the trajectory of a fascicle. For example, in the forceps minor, AD is low as the tract terminates at various targets within the frontal lobe and rises sharply as the tract forms a cohesive bundle while crossing the midline via the genu of the corpus callosum (Fig. 2). Similarly, RD is high in the thalamic radiation where the tract originates, but drops considerably as the tract enters the dense collection of myelinated white matter in the anterior limb of the internal capsule and rises again as the tract enters the cortical gray matter. Since these measurements were made in young children it is likely that some of the variation in diffusion properties is due to variation in the amount of myelin along the tract length as well (Dubois et al., 2006). In addition, white matter contains crossing, branching and merging fiber bundles and these geometric properties will have a substantial impact on the diffusion properties of a voxel (Jones, 2002). For example a bundle of axons that crosses through the main fascicle will hinder diffusion parallel to the fascicle but allow more diffusion perpendicular to the fascicle (Yeatman et al., 2012b). This will also lead to a reduction in fractional anisotropy. We believe that a portion of the variance in diffusion properties that we observe along the length of these fascicles is the product of crossing, merging and branching fibers.

The different tract profiles for AD, RD, MD and FA emphasize the importance of examining more than one diffusion parameters. For example, in the corticospinal tract, AD and RD are both elevated while the tract is within the brain stem. At this level, the corticospinal tract is mostly surrounded by transverse fibers of the pons which travel perpendicular to the corticospinal tracts. Partial voluming with these tracts likely produces the elevated RD seen at this point, which in combination with high AD, results in low FA values. AD values peak again where the corticospinal tract enters the internal capsule. However, radial diffusivity there remains low. This is likely because the corticospinal tract makes up the majority of the anterior portion of the posterior limb of the internal capsule resulting in less perpendicular diffusion. As a result, FA is highest at this point in the corticospinal tract. Patterns of variability within the four diffusion properties are informative in other tracts as well.

Sex differences in diffusion parameters

We found sexual dimorphism in portions of 4 tracts: the left cingulum, the right IFOF, the left ILF, and the right uncinate. The cingulum exhibited the most dramatic sex differences with significant effects for AD (males > females), RD (females > males) and FA (males > females; Fig. 3). Sexual dimorphism of cingulum diffusion parameters is seen in adults (Hsu et al., 2008; Huster et al., 2009; Rametti et al., 2011) and over lifespan development (Kochunov et al., 2012; Lebel and Beaulieu, 2011; Lebel et al., 2012; Trivedi et al., 2009). Consistent with the current data, the majority of reports find that FA is higher in males (but see Schneiderman et al., 2007) and the sexual dimorphism appears most often in the left cingulum. The cingulum is involved in attention, emotion and memory, and sexual dimorphisms in regions connected to the cingulum such as the cingulate cortex and the amygdala are also common (Biver et al., 1996; Giedd et al., 1997; Gur et al., 1995; Johnson et al., 2008; Merke et al., 2003; Paus et al., 1996; Pujol et al., 2002; Wrase et al., 2003).

Sexual dimorphism was also seen in the IFOF (Fig. 4). The IFOF has been linked to semantic understanding (Duffau, 2008), reading (Catani and Mesulam, 2008) and visual processing (Fox et al., 2008). Reduced mean RD in adult females has previously been reported in the right IFOF (Eluvathingal et al., 2007). Interestingly, increased FA in adult males has been reported in a voxel cluster near the location of

t4.1 **Table 4**
t4.2 Analysis of variation in diffusion properties along tract length.

t4.3	Effect of nodes				
t4.4	Tract name	AD	RD	MD	FA
t4.5	Left thalamic radiation	F = 1.11, p = 0.36	F = 5.17, p < 0.00*	F = 4.13, p < 0.00*	F = 2.27, p = 0.07
t4.6	Right thalamic radiation	F = 1.26, p = 0.28	F = 2.94, p = 0.02*	F = 2.87, p = 0.02*	F = 1.33, p = 0.26
t4.7	Left corticospinal	F = 3.59, p < 0.00*	F = 10.15, p < 0.00*	F = 10.45, p < 0.00*	F = 3.23, p = 0.01*
t4.8	Right corticospinal	F = 9.70, p < 0.00*	F = 16.91, p < 0.00*	F = 17.60, p < 0.00*	F = 6.58, p < 0.00*
t4.9	Left cingulum	F = 2.39, p = 0.03*	F = 2.99, p < 0.00*	F = 5.23, p = 0.01*	F = 0.78, p = 0.58
t4.10	Right cingulum	F = 1.69, p = 0.12	F = 4.04, p < 0.00*	F = 4.86, p < 0.00*	F = 2.06, p = 0.05*
t4.11	Forceps major	F = 2.44, p = 0.02*	F = 1.30, p = 0.03*	F = 1.52, p = 0.19	F = 1.63, p = 0.12
t4.12	Forceps minor	F = 2.24, p = 0.04*	F = 1.88, p = 0.10	F = 2.99, p = 0.01*	F = 0.84, p = 0.54
t4.13	Left inferior fronto-occipital	F = 1.30, p = 0.26	F = 0.30, p = 0.88	F = 0.52, p = 0.66	F = 0.99, p = 0.44
t4.14	Right inferior fronto-occipital	F = 1.85, p = 0.14	F = 1.94, p = 0.13	F = 1.86, p = 0.15	F = 2.34, p = 0.02*
t4.15	Left superior longitudinal	F = 0.63, p = 0.61	F = 1.18, p = 0.32	F = 1.32, p = 0.27	F = 0.75, p = 0.52
t4.16	Right superior longitudinal	F = 0.71, p = 0.55	F = 2.29, p = 0.08	F = 2.35, p = 0.08	F = 0.63, p = 0.39
t4.17	Left inferior longitudinal	F = 0.63, p = 0.63	F = 1.09, p = 0.37	F = 0.71, p = 0.59	F = 1.45, p = 0.21
t4.18	Right inferior longitudinal	F = 1.54, p = 0.19	F = 0.86, p = 0.50	F = 0.97, p = 0.42	F = 1.97, p = 0.06
t4.19	Left uncinate	F = 4.46, p < 0.00*	F = 1.13, p = 0.34	F = 3.77, p < 0.00*	F = 1.50, p = 0.19
t4.20	Right uncinate	F = 3.00, p = 0.02*	F = 2.04, p = 0.08	F = 3.62, p = 0.01*	F = 1.08, p = 0.37
t4.21	Left arcuate	F = 3.56, p < 0.00*	F = 0.95, p = 0.44	F = 3.40, p = 0.01*	F = 0.78, p = 0.57
t4.22	Right arcuate	F = 1.12, p = 0.35	F = 1.26, p = 0.28	F = 2.19, p = 0.05	F = 0.99, p = 0.43

t4.23 * Denotes a significant between node differences with p < 0.05.

457 the smaller band of sexually dimorphic AD seen in children (Fig. 4; 480
458 Rametti et al., 2011). While not identical to our results, these findings 481
459 suggest that sex differences persist in the IFOF. Furthermore, the large 482
460 posterior band of sex differences approximates the point where the 483
461 IFOF sharply radiates to eventual terminations in parietal, occipital 484
462 and posterior temporal cortices. There are sexual dimorphisms in 485
463 cortical thickness (females > males) in the right inferior parietal and 486
464 posterior temporal regions (Sowell et al., 2007), which may be related to 487
465 sexual dimorphism in this tract.

466 We also found a sex difference in FA within the left ILF (Fig. 5). The ILF 488
467 consists of long and short tracts with the more lateral short tracts 489
468 connecting adjacent nonpolar temporal gyri. The sex differences in FA 490
469 may be due to differing amounts of short tracts entering or exiting the 491
470 tract near the two bands of significant differences. Overall RD and MD 492
471 are lower in the ILF of adolescent females compared with males 493
472 (Eluvathingal et al., 2007), and two previous lifespan reports also found 494
473 sex differences in ILF FA with the same (Hasan et al., 2010) and opposite 495
474 (Lebel et al., 2012) direction as the current data (male FA > female). Face 496
475 recognition and emotional memory which are associated with the ILF 497
476 and its connected regions (Fox et al., 2008; Philippi et al., 2009) also sex- 498
477 ually dimorphic with women outperforming men on face recognition 499
478 and emotional memory tasks (Cahill et al., 1996; Cellerino et al., 2004; 500
479 Lewin and Herlitz, 2002).

480 The right uncinate fasciculus was sexually dimorphic as well (Fig. 5). 480
481 Two other lifespan studies starting at 5 years found higher mean FA in 481
482 the uncinate fasciculus of males compared with females suggesting 482
483 that this sex difference is persistent (Lebel and Beaulieu, 2011; Lebel 483
484 et al., 2012). Like the SLF and cingulum, the uncinate connects polar 484
485 temporal lobe areas, including the amygdala, to cortical regions. Inter- 485
486 estingly, a study examining 12-year-old male and female children 486
487 born preterm found a group by sex interaction using ROI analysis of 487
488 the right uncinate fasciculus. In control participants, males had higher 488
489 FA compared with females, but in the preterm group, males had lower 489
490 FA. Verbal IQ and Peabody Picture Vocabulary Test-Revised scores 490
491 were correlated with both right and left uncinate fasciculus scores in 491
492 the preterm male group (Constable et al., 2008).

493 These findings demonstrate that multiple fiber tract diffusion param- 493
494 eter sexual dimorphisms are present in young children. The overall 494
495 pattern of tract differences suggest sexual dimorphism in connections 495
496 between visual and emotion/memory centers (ILF), visual and higher- 496
497 order processing centers (IFOF), emotion/memory centers and higher- 497
498 order processing centers (uncinate, cingulum). Most of the cortical 498
499 and sub-cortical targets of these tracts are sexually dimorphic in adults 499
500 and exhibit high levels of steroid hormone receptor concentration in 500
501 animal models (see Goldstein et al., 2001). We suspect that these tract 501
502 sexual dimorphisms are the result of organizational actions of steroid 502

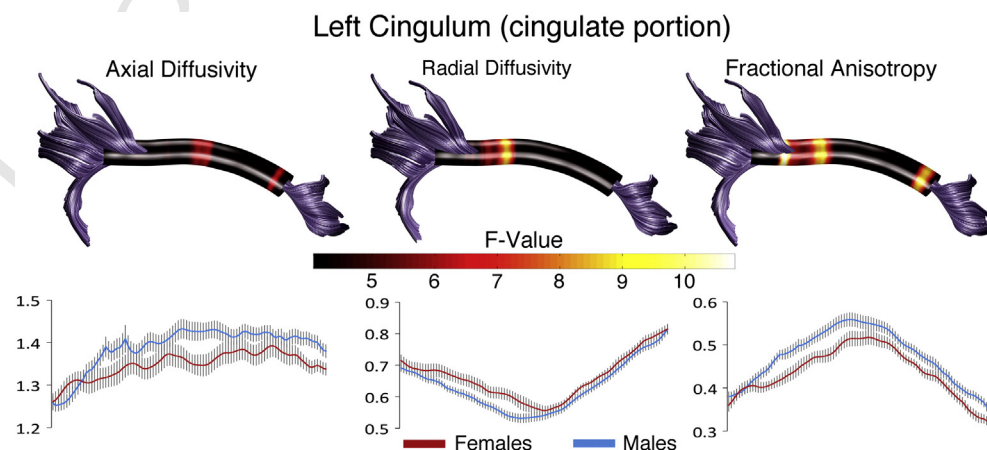


Fig. 3. Sex differences in the left cingulate portion of the cingulum. Tract profiles illustrating sex differences in AD, RD, and FA along the cingulum in typically developing male and female children. Color bar indicates F statistic values from Bonferroni-corrected analyses of covariance conducted at each location along the tract length. Significant comparisons are indicated by non-black regions. Plots for AD, RD and FA in males and females are presented below each tract profile.

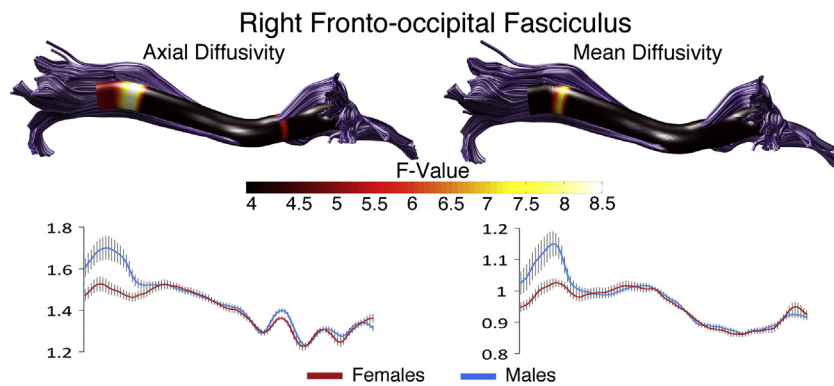


Fig. 4. Sex differences in the right inferior fronto-occipital fasciculus. Tract profiles illustrating sex differences in AD and MD along the right OFF in typically developing male and female children. Color bar indicates F statistic values from Bonferroni-corrected analyses of covariance conducted at each location along the tracts length. Significant comparisons are indicated by non-black regions. Plots for AD and MD in males and females are presented below each tract profile.

hormones or sex chromosome genetics occurring in utero or during the perinatal hormone surge.

In addition, these sex differences are concentrated in select locations along the tracts. One possible explanation is that hormone sensitive gray matter regions produce sexually dimorphic axonal contributions to these tracts which manifest in diffusion parameter differences at these locations. Alternately, diffusion parameter sexual dimorphisms may be due to greater tract curvature or partial voluming with adjacent structures or even different rates of tract myelination. Sexual differentiation studies incorporating localized measures of diffusion in both younger and older children will produce a map of white matter sexual dimorphism emergence, which may be useful in understanding disorders with sex biases in the population.

Age effects in diffusion parameters

Age is known to be an important factor in measures of white matter diffusion. The few neonatal DTI studies available show considerable change in fiber tract diffusion parameters during neonatal life, but the rate of change appears to slow past 24 months (Hermoye et al., 2006; Huang et al., 2006; Trivedi et al., 2009). Lifespan development studies starting from age 5 describe increases in FA followed by a plateau for most tracts during early adulthood and a slow decline during old age with an opposite pattern for MD (Eluvathingal et al., 2007; Lebel and Beaulieu, 2011; Lebel et al., 2008, 2012; Schmithorst, 2009). Similar to results in older children, we found generally positive relationships between age and FA (Fig. 6; left IFOF, right arcuate) and mostly negative relationships between age and MD (Fig. 6; forceps minor, left uncinate).

Increasing FA with age is thought to be driven by decreasing RD as white matter become increasingly myelinated (Bonekamp et al., 2007; Eluvathingal et al., 2007; Hasan et al., 2010; Verhoeven et al., 2009; Westlye et al., 2010). This was the case in the right arcuate where RD and FA displayed opposing correlations with age. In the left IFOF, the only other tract to show a significant age effect for FA, the effect of age on RD approached significance for RD ($p = 0.069$).

The current data help bridge the age gap in our understanding of white matter in children and provide additional details in several tracts by illustrating that aging does not uniformly influence tract diffusion parameters. We suspect that other tracts undergo similar age-related changes along their length but the restricted age range in our participants, spanning 26–46 months, reduced the number of age effects in the omnibus tests. Longitudinal analysis using AFQ will clarify patterns in tract maturation with a new level of detail.

Laterality in diffusion parameters

Similar to sexual dimorphism, asymmetry in white-matter diffusion parameters is region specific and age-dependent (Ardekani et al., 2007; Bonekamp et al., 2007; Hasan et al., 2010; Liu et al., 2010; Trivedi et al., 2009). Studies in very young children suggest left-ward asymmetries with higher fractional anisotropy in the left corticospinal tract, left superior longitudinal fasciculus, left arcuate fasciculus and possibly the left thalamic radiations (Dubois et al., 2009; Liu et al., 2010). Lifespan development reports (mostly starting above age 5) also suggest a mild left-ward asymmetry in overall FA but with few significant comparisons among specific tracts (Lebel et al., 2012; Trivedi et al., 2009). We found diffusion parameter asymmetries in 9 of the 10 tract pairs/sides

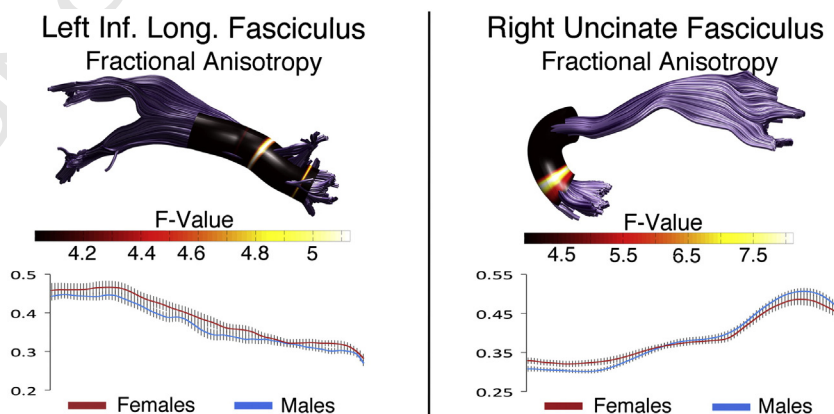


Fig. 5. Sex differences in the left superior longitudinal fasciculus and right uncinate fasciculus. Tract profiles illustrating sex differences in FA along the left ILF and right uncinate in typically developing male and female children. Color bar indicates F statistic values from Bonferroni-corrected analyses of covariance conducted at each location along the tracts length. Significant comparisons are indicated by non-black regions. Corresponding plots for FA in males and females are presented below each tract profile.

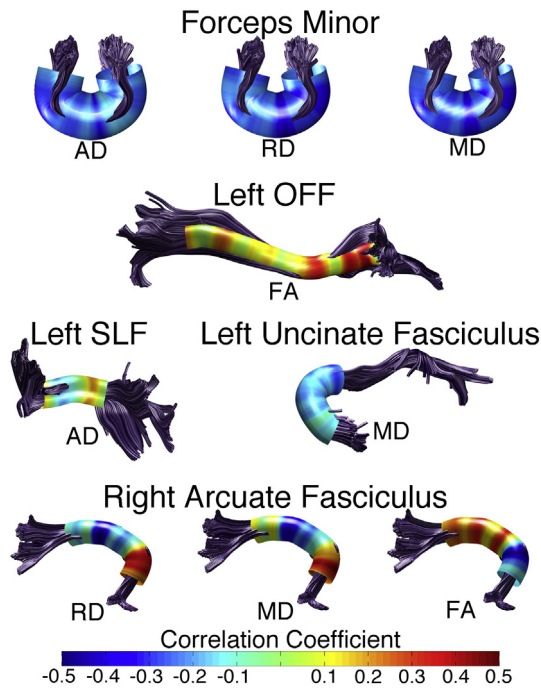


Fig. 6. Relationship between participant age and diffusion parameters in several tracts. Tract profiles illustrating partial correlations between age and various diffusion parameters in tracts where age emerged as a significant covariate. Scanner type and handedness are controlled. Correlation strength was variable along the tract. Colors represent the strength of the relationship as indicated by r -values. Warmer colors indicate a positive relationship and cooler colors indicate a negative one.

examined (Fig. 2, Table 3). Several of these asymmetries have been reported in adults (Bonekamp et al., 2007; Büchel et al., 2004; Thiebaut de Schotten et al., 2011; Westerhausen et al., 2007) and leftward asymmetries in the arcuate fasciculus and cingulum are especially prevalent.

Mean FA and tract density are greater in the left arcuate fasciculus compared with the right in adults and older children (Büchel et al., 2004; Dubois et al., 2009; Fletcher et al., 2010; Lebel and Beaulieu, 2009; Paus et al., 1999; Powell et al., 2006; Rodrigo et al., 2007). We also observed asymmetry of arcuate FA in younger children (Fig. 2). In

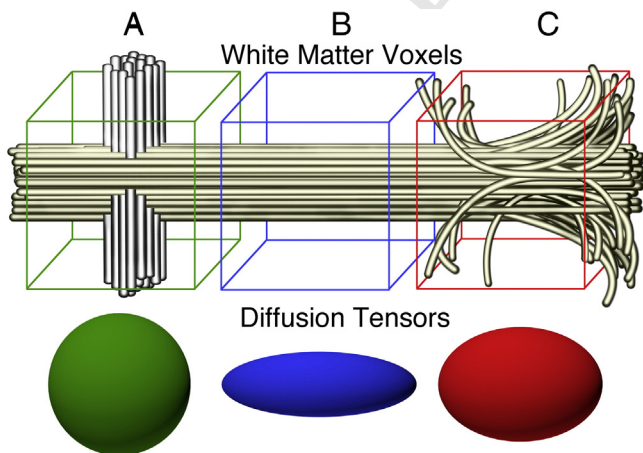


Fig. 7. Environmental contributions to tract anisotropy. Variations in diffusion parameters along tracts during normative development are likely a combination of tract specific (myelin content, axonal integrity) and local environment contributions. Voxel A contains a tract of interest (yellow) as well as a crossing tract (gray), resulting in low anisotropy measurements at this point. Voxel B contains only the tract of interest and exhibits high anisotropy. Within voxel C axons from nearby gray matter join the tract and some axons break off heading towards gray matter targets. The result would be a drop in anisotropy measurements at this point in the tract.

agreement with Fletcher et al.'s (2010) description in typically developing adolescent boys, we also found higher MD and RD in the right arcuate compared with the left (Table 3). Asymmetry in the arcuate fasciculi is linked to faster maturation in the left arcuate due to the important role it plays in that hemisphere's language circuit (Klingberg et al., 2000; Rauschecker et al., 2009; Rolheiser et al., 2011; Yeatman et al., 2011).

A second consistent asymmetry is a leftward bias in cingulum FA which is robust and present over the lifespan (Bonekamp et al., 2007; Gong et al., 2005a, 2005b; Trivedi et al., 2009; Wilde et al., 2009). We confirmed higher mean FA in the left cingulum of children and show that this is the product of higher AD in the left cingulum and higher RD in the right cingulum (Fig. 2). The greater AD in the left and greater RD in the right cingulum suggest a more cohesive tract bundle with possibly greater axonal density and myelination in the left hemisphere.

Several of the cingulum's gray matter targets such as the cingulate cortex and amygdala also exhibit considerable laterality (Andersen and Teicher, 1999; Cooke et al., 2007; Gasbarri et al., 2007; Giedd et al., 1997; Huster et al., 2007; Johnson et al., 2008; Killgore et al., 2001; Paus et al., 1996; Scicli et al., 2004; Yücel et al., 2001), and laterality in anterior cingulate gray matter has been linked to personality, executive-control, and risk for psychotic illness (Fornito et al., 2004; Pujol et al., 2002; Yücel et al., 2003). The current data illustrate that the cingulum, which receives contributions from both the amygdala and cingulate cortex, is also asymmetric from a young age in humans.

Limitations

The current study provides a new level of detail regarding white matter diffusion parameters in young children, but there are a few issues to note. Although AFQ provides a method to assess within tract variance, the use of a tensor models means that we do not trace the trajectory of fiber tracts crossing the principle tract bundle in a voxel. This means that we measure the core of a tract but do not measure all of its smaller branches. Relatedly, diffusion parameters were not measured at the extremes of each tract near the cortical endpoints. Measuring in these areas may provide useful information but will likely also be subject to extremely high levels of variability due to partial voluming with gray matter. Additionally, because AFQ tracts fibers in native space, due to individual variability in factors such as tract curvature, tract size, and image quality, some tracts entered statistical analysis with a greater sample size than others (Table 2). Additional analysis of the right cingulum and right arcuate, the only tracts with fewer than 50 subjects might identify additional within or between subjects effects in these tracts. Finally, because the current data are part of a larger longitudinal study taking place over several years, improvements to the research center's scanner software occurred during data collection. To account for this, we have included scanner status as a covariate in our analyses. While there were differences in fiber identification rates (Table 2) the between-subjects factor in our model (participant sex) was not differentially distributed among the two scanner statuses (Fisher's exact test, $p = 0.62$).

Conclusions

Our results indicate that in young children, factors such as within-tract variability, sex, hemisphere and age exhibit variable influence on diffusion parameters along the major fasciculi. These findings also illustrate how repeated sampling of multiple diffusion parameters produces a more detailed understanding of a tract than mean measures of a single descriptor such as fractional anisotropy and mean diffusivity. Normal variation in tract diffusion parameters can be caused by gross properties such as tract curvature and partial voluming with nearby structures but may also illustrate changes in local myelination, axonal density and/or the addition and elimination of axons to the tract. Given the highly variable patterns of correlation between age and diffusion parameters

along the tract length, longitudinal studies describing changes to the diffusion parameter profile of a tract are particularly informative.

The present study provides an enhanced level of detail regarding sexual dimorphism and hemispheric asymmetry in tract diffusion properties. Abnormal cerebral asymmetry has been linked to intellectual deficits and schizophrenia (Burns et al., 2003; Crow, 2004; Rosenberger and Hier, 1980; Wang et al., 2004) and disorders such as autism and depression exhibit pronounced sex biases in the population. A more thorough understanding of how sexual dimorphism and hemispheric asymmetry influence major fasciculi in normative development may improve our ability to identify white matter abnormalities in several disorders.

Acknowledgments

The authors would like to thank Shae DiNino, Kayla Harrington, Aaron Lee, Deana Li, Sarah Liston and Mark Shen for technical assistance in data collection and processing. We also thank Sally Rogers, Sally Ozonoff and Lesley Deprey for collection and assistance in interpreting handedness data, all of the APP staff involved in the logistics of the study, and all the families who participated in the Autism Phenome Q17 Project.

References

Andersen, S.L., Teicher, M.H., 1999. Serotonin laterality in amygdala predicts performance in the elevated plus maze in rats. *Neuroreport* 10, 3497.

Ardekani, S., Kumar, A., Bartzokis, G., Sinha, U., 2007. Exploratory voxel-based analysis of diffusion indices and hemispheric asymmetry in normal aging. *Magn. Reson. Imaging* 25, 154–167.

Beaulieu, C., 2002. The basis of anisotropic water diffusion in the nervous system – a technical review. *NMR Biomed.* 15, 435–455.

Biver, F., Lotstra, F., Monclus, M., Wikler, D., Damhaut, P., Mendlewicz, J., Goldman, S., 1996. Sex difference in 5HT₂ receptor in the living human brain. *Neurosci. Lett.* 204, 25–28.

Bonekamp, D., Nagae, L.M., Degaonkar, M., Matson, M., Abdalla, W.M.A., Barker, P.B., Mori, S., Horska, A., 2007. Diffusion tensor imaging in children and adolescents: reproducibility, hemispheric, and age-related differences. *Neuroimage* 34, 733–742.

Büchel, C., Raedler, T., Sommer, M., Sach, M., Weiller, C., Koch, M.A., 2004. White matter asymmetry in the human brain: a diffusion tensor MRI study. *Cereb. Cortex* 14, 945–951.

Burns, J., Job, D., Bastin, M.E., Whalley, H., Macgillivray, T., Johnstone, E.C., Lawrie, S.M., 2003. Structural disconnection in schizophrenia: a diffusion tensor magnetic resonance imaging study. *Br. J. Psychiatry* 182, 439–443.

Cahill, L.F., Haier, R., Fallon, J., 1996. Amygdala activity at encoding correlated with long-term, free recall of emotional information. *Proc. Natl. Acad. Sci. U. S. A.* 93, 8016–8021.

Catani, M., Mesulam, M., 2008. The arcuate fasciculus and the disconnection theme in language and aphasia: history and current state. *Cortex* 44, 953–961.

Catani, M., Allin, M.P.G., Husain, M., Pugliese, L., Mesulam, M.M., Murray, R.M., Jones, D.K., 2007. Symmetries in human brain language pathways correlate with verbal recall. *Proc. Natl. Acad. Sci. U. S. A.* 104, 17163–17168.

Cellerino, A., Borghetti, D., Sartucci, F., 2004. Sex differences in face gender recognition in humans. *Brain Res. Bull.* 63, 443–449.

Chang, L.-C., Jones, D.K., Pierpaoli, C., 2005. RESTORE: robust estimation of tensors by outlier rejection. *Magn. Reson. Med.* 53, 1088–1095.

Choi, C.-H., Lee, J.-M., Koo, B.-B., Park, J.S., Kim, D.-S., Kwon, J.S., Kim, I.Y., 2010. Sex differences in the temporal lobe white matter and the corpus callosum: a diffusion tensor tractography study. *Neuroreport* 21, 73–77.

Constable, R.T., Ment, L.R., Vohr, B.R., Kesler, S.R., Fulbright, R.K., Lacadie, C., Delancy, S., Katz, K.H., Schneider, K.C., Schafer, R.J., Makuch, R.W., Reiss, A.R., 2008. Prematurely born children demonstrate white matter microstructural differences at 12 years of age, relative to term control subjects: an investigation of group and gender effects. *Pediatrics* 121, 306–316.

Cooke, B.M., Stokas, M.R., Woolley, C.S., 2007. Morphological sex differences and laterality in the prepubertal medial amygdala. *J. Comp. Neurol.* 501, 904–915.

Crow, T.J., 2004. Cerebral asymmetry and the lateralization of language: core deficits in schizophrenia as pointers to the gene. *Curr. Opin. Psychiatry* 17, 97.

Dubois, J., Hertz-Pannier, L., Dehaene-Lambertz, G., 2006. Assessment of the early organization and maturation of infants' cerebral white matter fiber bundles: a feasibility study using quantitative diffusion tensor imaging and tractography. *Neuroimage* 30, 1121–1132.

Dubois, J., Hertz-Pannier, L., Cachia, A., Mangin, J.F., Le Bihan, D., Dehaene-Lambertz, G., 2009. Structural asymmetries in the infant language and sensori-motor networks. *Cereb. Cortex* 19, 414–423.

Duffau, H., 2008. The anatomo-functional connectivity of language revisited. *Neuropsychologia* 46, 927–934.

Eluvathingal, T.J., Hasan, K.M., Kramer, L., Fletcher, J.M., Ewing-Cobbs, L., 2007. Quantitative diffusion tensor tractography of association and projection fibers in normally developing children and adolescents. *Cereb. Cortex* 17, 2760–2768.

Fletcher, P.T., Whitaker, R.T., Tao, R., DuBray, M.B., Froehlich, A., Ravichandran, C., Alexander, A.L., Bigler, E.D., Lange, N., Lainhart, J.E., 2010. Microstructural connectivity of the arcuate fasciculus in adolescents with high-functioning autism. *Neuroimage* 51, 1117–1125.

Fornito, A., Yücel, M., Wood, S., Stuart, G.W., Buchanan, J.-A., Proffitt, T., Anderson, V., Velakoulis, D., Pantelis, C., 2004. Individual differences in anterior cingulate/paracingulate morphology are related to executive functions in healthy males. *Cereb. Cortex* 14, 424–431.

Fox, C.J., Iaria, G., Barton, J.J.S., 2008. Disconnection in prosopagnosia and face processing. *Cortex* 44, 996–1009.

Gabrieli, J.D.E., 2009. Dyslexia: a new synergy between education and cognitive neuroscience. *Science* 325, 280–283.

Gasbarri, A., Arnone, B., Pompili, A., Pacitti, F., Pacitti, C., Cahill, L.F., 2007. Sex-related hemispheric lateralization of electrical potentials evoked by arousing negative stimuli. *Brain Res.* 1138, 178–186.

Giedd, J.N., Snell, J.W., Lange, N., Rajapakse, J.C., Casey, B.J., Kozuch, P.L., Vaituzis, A.C., Vauss, Y.C., Hamburger, S.D., Kaysen, D., Rapoport, J.L., 1996. Quantitative magnetic resonance imaging of human brain development: ages 4–18. *Cereb. Cortex* 6, 551–559.

Giedd, J.N., Castellanos, F.X., Rajapakse, J.C., Vaituzis, A.C., Rapoport, J.L., 1997. Sexual dimorphism of the developing human brain. *Prog. Neuropsychopharmacol. Biol. Psychiatry* 21, 1185–1201.

Gilmore, J.H., Lin, W., Prastawa, M., 2007. Regional gray matter growth, sexual dimorphism, and cerebral asymmetry in the neonatal brain. *J. Neurosci.* 27, 1255–1260.

Gilmore, J.H., Shi, F., Woolson, S.L., Knickmeyer, R.C., Short, S.J., Lin, W., Zhu, H., Hamer, R.M., Styner, M., Shen, D., 2012. Longitudinal development of cortical and subcortical gray matter from birth to 2 years. *Cereb. Cortex* 22, 2478–2485.

Goldstein, J.M., Seidman, L.J., Horton, N.J., Makris, N., Kennedy, D.N., Caviness Jr., V.S., Faraone, S.V., Tsuang, M.T., 2001. Normal sexual dimorphism of the adult human brain assessed by in vivo magnetic resonance imaging. *Cereb. Cortex* 11, 490–497.

Gong, G., Jiang, T., Zhu, C., Zang, Y., He, Y., Xie, S., Xiao, J., 2005a. Side and handedness effects on the cingulum from diffusion tensor imaging. *Neuroreport* 16, 1701.

Gong, G., Jiang, T., Zhu, C., Zang, Y., Wang, F., Xie, S., Xiao, J., Guo, X., 2005b. Asymmetry analysis of cingulum based on scale-invariant parameterization by diffusion tensor imaging. *Hum. Brain Mapp.* 24, 92–98.

Goodlett, C.B., Fletcher, P.T., Gilmore, J.H., Gerig, G., 2009. Group analysis of DTI fiber tract statistics with application to neurodevelopment. *Neuroimage* 45, S133–S142.

Greenhouse, S.W., Geisser, S., 1959. On methods in the analysis of profile data. *Psychometrika* 24, 95–112.

Gur, R.C., Mozley, L.H., Mozley, P.D., Resnick, S.M., Karp, J.S., Alavi, A., Arnold, S.E., Gur, R.E., 1995. Sex differences in regional cerebral glucose metabolism during a resting state. *Science* 267, 528–531.

Hasan, K.M., Kamali, A., Abid, H., Kramer, L.A., Fletcher, J.M., Ewing-Cobbs, L., 2010. Quantification of the spatiotemporal microstructural organization of the human brain association, projection and commissural pathways across the lifespan using diffusion tensor tractography. *Brain Struct. Funct.* 214, 361–373.

Hermoye, L., Saint-Martin, C., Cosnard, G., Lee, S.-K., Kim, J., Nassogne, M.-C., Menten, R., Clapuyt, P., Donohue, P.K., Hua, K., Wakana, S., Jiang, H., van Zijl, P.C.M., Mori, S., 2006. Pediatric diffusion tensor imaging: normal database and observation of the white matter maturation in early childhood. *Neuroimage* 29, 493–504.

Honea, R., Crow, T.J., Passingham, D., Mackay, C.E., 2005. Regional deficits in brain volume in schizophrenia: a meta-analysis of voxel-based morphometry studies. *Am. J. Psychiatry* 162, 2233–2245.

Hsu, J.L., Leemans, A., Bai, C.H., Lee, C.H., Tsai, Y.F., Chiu, H.C., Chen, W.H., 2008. Gender differences and age-related white matter changes of the human brain: a diffusion tensor imaging study. *Neuroimage* 39, 566–577.

Huang, H., Zhang, J., Wakana, S., Zhang, W., Ren, T., Richards, L.J., Yarowsky, P., Donohue, P.K., Graham, E., van Zijl, P.C.M., Mori, S., 2006. White and gray matter development in human fetal, newborn and pediatric brains. *Neuroimage* 33, 27–38.

Huster, R.J., Westerhausen, R., Kreuder, F., Schweiger, E., Wittling, W., 2007. Morphologic asymmetry of the human anterior cingulate cortex. *Neuroimage* 34, 888–895.

Huster, R.J., Westerhausen, R., Kreuder, F., Schweiger, E., Wittling, W., 2009. Hemispheric and gender related differences in the midcingulum bundle: a DTI study. *Hum. Brain Mapp.* 30, 383–391.

Huttenlocher, P.R., Dabholkar, A.S., 1997. Regional differences in synaptogenesis in human cerebral cortex. *J. Comp. Neurol.* 387, 167–178.

Jernigan, T.L., Hesselink, J.R., Sowell, E., Tallal, P.A., 1991. Cerebral structure on magnetic resonance imaging in language- and learning-impaired children. *Arch. Neurol.* 48, 539–545.

Johnson, R., Breedlove, S.M., Jordan, C.L., 2008. Sex differences and laterality in astrocyte number and complexity in the adult rat medial amygdala. *J. Comp. Neurol.* 511, 599–609.

Jones, D.K., 2002. Determining and visualizing uncertainty in estimates of fiber orientation from diffusion tensor MRI. *Magn. Reson. Med.* 49, 7–12.

Killgore, W.D., Oki, M., Yurgelun-Todd, D.A., 2001. Sex-specific developmental changes in amygdala responses to affective faces. *Neuroreport* 12, 427–433.

Kim, J.H., Loy, D.N., Liang, H.-F., Trinkaus, K., Schmidt, R.E., Song, S.-K., 2007. Noninvasive diffusion tensor imaging of evolving white matter pathology in a mouse model of acute spinal cord injury. *Magn. Reson. Med.* 58, 253–260.

Klingberg, T., Hedehus, M., Temple, E., Salz, T., Gabrieli, J.D., Moseley, M.E., Poldrack, R.A., 2000. Microstructure of temporo-parietal white matter as a basis for reading ability: evidence from diffusion tensor magnetic resonance imaging. *Neuron* 25, 493–500.

Knickmeyer, R.C., Gouttard, S., Kang, C., Evans, D., Wilber, K., Smith, J.K., Hamer, R.M., Lin, W., Gerig, G., Gilmore, J.H., 2008. A structural MRI study of human brain development from birth to 2 years. *J. Neurosci.* 28, 12176–12182.

- Kochunov, P., Williamson, D.E., Lancaster, J., Fox, P., Cornell, J., Blangero, J., Glahn, D.C., 2012. Fractional anisotropy of water diffusion in cerebral white matter across the lifespan. *Neurobiol. Aging* 33, 9–20.
- Lebel, C., Beaulieu, C., 2009. Lateralization of the arcuate fasciculus from childhood to adulthood and its relation to cognitive abilities in children. *Hum. Brain Mapp.* 30, 3563–3573.
- Lebel, C., Beaulieu, C., 2011. Longitudinal development of human brain wiring continues from childhood into adulthood. *J. Neurosci.* 31, 10937–10947.
- Lebel, C., Walker, L., Leemans, A., Phillips, L., Beaulieu, C., 2008. Microstructural maturation of the human brain from childhood to adulthood. *Neuroimage* 40, 1044–1055.
- Lebel, C., Gee, M., Camicioli, R., Wielar, M., Martin, W., Beaulieu, C., 2012. Diffusion tensor imaging of white matter tract evolution over the lifespan. *Neuroimage* 60, 340–352.
- Lewin, C., Herlitz, A., 2002. Sex differences in face recognition—Women's faces make the difference. *Brain Cogn.* 50, 121–128.
- Liu, Y., Balériaux, D., Kavc, M., Metens, T., Absil, J., Denolin, V., Pardou, A., Avni, F., Van Bogaert, P., Aeby, A., 2010. Structural asymmetries in motor and language networks in a population of healthy preterm neonates at term equivalent age: a diffusion tensor imaging and probabilistic tractography study. *Neuroimage* 51, 783–788.
- Mauchly, J.W., 1940. Significance test for sphericity of a normal n-variate distribution. *Ann. Math. Stat.* 11, 204–209.
- Merke, D.P., Fields, J.D., Keil, M.F., Vaituzis, A.C., Chrousos, G.P., Giedd, J.N., 2003. Children with classic congenital adrenal hyperplasia have decreased amygdala volume: potential prenatal and postnatal hormonal effects. *J. Clin. Endocrinol. Metab.* 88, 1760–1765.
- Mishra, A., Anderson, A.W., Wu, X., Gore, J.C., Ding, Z., 2010. An improved Bayesian tensor regularization and sampling algorithm to track neuronal fiber pathways in the language circuit. *Med. Phys.* 37, 4274–4287.
- Nordahl, C.W., Simon, T.J., Zierhut, C., Solomon, M., Rogers, S.J., Amaral, D.G., 2008. Brief report: methods for acquiring structural MRI data in very young children with autism without the use of sedation. *J. Autism Dev. Disord.* 38, 1581–1590.
- Nordahl, C.W., Lange, N., Li, D.D., Barnett, L.A., Lee, A., Buonocore, M.H., Simon, T.J., Rogers, S., Ozonoff, S., Amaral, D.G., 2011. Brain enlargement is associated with regression in preschool-age boys with autism spectrum disorders. *Proc. Natl. Acad. Sci. U. S. A.* 108, 20195–20200.
- Nordahl, C.W., Scholz, R., Yang, X., Buonocore, M.H., Simon, T., Rogers, S., Amaral, D.G., 2012. Increased rate of amygdala growth in children aged 2 to 4 years with autism spectrum disorders: a longitudinal study. *Arch. Gen. Psychiatry* 69, 53–61.
- Paus, T., Otaky, N., Caramanos, Z., MacDonald, D., Zijdenbos, A., D'Avirro, D., Gutmans, D., Holmes, C., Tomaiuolo, F., Evans, A.C., 1996. In vivo morphometry of the intrasulcal gray matter in the human cingulate, paracingulate, and superior-rostral sulci: hemispheric asymmetries, gender differences and probability maps. *J. Comp. Neurol.* 376, 664–673.
- Paus, T., Zijdenbos, A., Worsley, K., Collins, D.L., Blumenthal, J., Giedd, J.N., Rapoport, J.L., Evans, A.C., 1999. Structural maturation of neural pathways in children and adolescents: in vivo study. *Science* 283, 1908–1911.
- Peterson, B.S., 2003. Brain imaging studies of the anatomical and functional consequences of preterm birth for human brain development. *Ann. N. Y. Acad. Sci.* 1008, 219–237.
- Pfefferbaum, A., Mathalon, D.H., Sullivan, E.V., Rawles, J.M., Zipursky, R.B., Lim, K.O., 1994. A quantitative magnetic resonance imaging study of changes in brain morphology from infancy to late adulthood. *Arch. Neurol.* 51, 874–887.
- Philippi, C.L., Mehta, S., Grabowski, T., Adolphs, R., Rudrauf, D., 2009. Damage to association fiber tracts impairs recognition of the facial expression of emotion. *J. Neurosci.* 29, 15089–15099.
- Pierpaoli, C., Basser, P.J., 1996. Toward a quantitative assessment of diffusion anisotropy. *Magn. Reson. Med.* 36, 893–906.
- Powell, H.W.R., Parker, G.J.M., Alexander, D.C., Symms, M.R., Boulby, P.A., Wheeler-Kingshott, C.A.M., Barker, G.J., Noppeney, U., Koeppe, M.J., Duncan, J.S., 2006. Hemispheric asymmetries in language-related pathways: a combined functional MRI and tractography study. *Neuroimage* 32, 388–399.
- Pujol, J., López, A., Deus, J., Cardoner, N., Vallejo, J., Capdevila, A., Paus, T., 2002. Anatomical variability of the anterior cingulate gyrus and basic dimensions of human personality. *Neuroimage* 15, 847–855.
- Qiu, D., Tan, L.-H., Zhou, K., Khong, P.-L., 2008. Diffusion tensor imaging of normal white matter maturation from late childhood to young adulthood: voxel-wise evaluation of mean diffusivity, fractional anisotropy, radial and axial diffusivities, and correlation with reading development. *Neuroimage* 41, 223–232.
- Qiu, A., Fortier, M.V., Bai, J., Zhang, X., Chong, Y.-S., Kwek, K., Saw, S.-M., Godfrey, K.M., Gluckman, P.D., Meaney, M.J., 2013. Morphology and microstructure of subcortical structures at birth: a large-scale Asian neonatal neuroimaging study. *Neuroimage* 65, 315–323.
- Rametti, G., Carrillo, B., Gómez-Gil, E., Junque, C., Zubiarré-Elorza, L., Segovia, S., Gomez, Á., Guillamon, A., 2011. The microstructure of white matter in male to female transsexuals before cross-sex hormonal treatment A DTI study. *J. Psychiatry Res.* 45, 949–954.
- Rauschecker, A.M., Deutsch, G.K., Ben-Shachar, M., Schwartzman, A., Perry, L.M., Dougherty, R.F., 2009. Reading impairment in a patient with missing arcuate fasciculus. *Neuropsychologia* 47, 180–194.
- Rodrigo, S., Naggara, O., Oppenheim, C., Golestani, N., Poupon, C., Cointepas, Y., Mangin, J.F., Le Bihan, D., Meder, J.F., 2007. Human subinsular asymmetry studied by diffusion tensor imaging and fiber tracking. *Am. J. Neuroradiol.* 28, 1526–1531.
- Rolheiser, T., Stamatakis, E.A., Tyler, L.K., 2011. Dynamic processing in the human language system: synergy between the arcuate fascicle and extreme capsule.
- Rosenberger, P.B., Hier, D.B., 1980. Cerebral asymmetry and verbal intellectual deficits. *Ann. Neurol.* 8, 300–304.
- Schmithorst, V.J., 2009. Developmental sex differences in the relation of neuroanatomical connectivity to intelligence. *Intelligence* 37, 164–173.
- Schmithorst, V.J., Holland, S.K., Dardzinski, B.J., 2008. Developmental differences in white matter architecture between boys and girls. *Hum. Brain Mapp.* 29, 696–710.
- Schneiderman, J.S., Buchsbaum, M.S., Haznedar, M.M., Hazlett, E.A., Brickman, A.M., Shihabuddin, L., Brand, J.G., Torosjan, Y., Newmark, R.E., Tang, C., Aronowitz, J., Paul-Oudouard, R., Byne, W., Hof, P.R., 2007. Diffusion tensor anisotropy in adolescents and adults. *Neuropsychobiology* 55, 96–111.
- Scicli, A.P., Petrovich, G.D., Swanson, L.W., Thompson, R.F., 2004. Contextual fear conditioning is associated with lateralized expression of the immediate early gene c-fos in the central and basolateral amygdalar nuclei. *Behav. Neurosci.* 118, 5–14.
- Sled, J.G., Zijdenbos, A.P., Evans, A.C., 1998. A nonparametric method for automatic correction of intensity nonuniformity in MRI data. *IEEE Trans. Med. Imaging* 17, 87–97.
- Smith, S.M., 2002. Fast robust automated brain extraction. *Hum. Brain Mapp.* 17, 143–155.
- Song, S.-K., Sun, S.-W., Ramsbottom, M.J., Chang, C., Russell, J., Cross, A.H., 2002. Demyelination revealed through MRI as increased radial (but unchanged axial) diffusion of water. *Neuroimage* 17, 1429–1436.
- Song, S.-K., Sun, S.-W., Ju, W.-K., Lin, S.-J., Cross, A.H., Neufeld, A.H., 2003. Diffusion tensor imaging detects and differentiates axon and myelin degeneration in mouse optic nerve after retinal ischemia. *Neuroimage* 20, 1714–1722.
- Sowell, E.R., Peterson, B.S., Kan, E., Woods, R.P., Yoshii, J., Bansal, R., Xu, D., Zhu, H., Thompson, P.M., Toga, A.W., 2007. Sex differences in cortical thickness mapped in 176 healthy individuals between 7 and 87 years of age. *Cereb. Cortex* 17, 1550–1560.
- Sun, S.-W., Liang, H.-F., Trinkaus, K., Cross, A.H., Armstrong, R.C., Song, S.-K., 2006. Noninvasive detection of cuprizone induced axonal damage and demyelination in the mouse corpus callosum. *Magn. Reson. Med.* 55, 302–308.
- Thiebaut de Schotten, M., Ffytche, D.H., Bizzi, A., Dell'acqua, F., Allin, M., Walshe, M., Murray, R., Williams, S.C., Murphy, D.G.M., Catani, M., 2011. Atlasing location, asymmetry and inter-subject variability of white matter tracts in the human brain with MR diffusion tractography. *Neuroimage* 54, 49–59.
- Thomalla, G., Glauche, V., Koch, M.A., Beaulieu, C., Weiller, C., Röther, J., 2004. Diffusion tensor imaging detects early Wallerian degeneration of the pyramidal tract after ischemic stroke. *Neuroimage* 22, 1767–1774.
- Trivedi, R., Agarwal, S., Rathore, R.K.S., Saksena, S., Tripathi, R.P., Malik, G.K., Pandey, C.M., Gupta, R.K., 2009. Understanding development and lateralization of major cerebral fiber bundles in pediatric population through quantitative diffusion tensor tractography. *Pediatr. Res.* 66, 636–641.
- Tyszk, J.M., Readhead, C., Bearer, E.L., Pautler, R.G., Jacobs, R.E., 2006. Statistical diffusion tensor histology reveals regional dysmyelination effects in the shiverer mouse mutant. *Neuroimage* 29, 1058–1065.
- Verhoeven, J.S., Sage, C.A., Leemans, A., Van Hecke, W., Callaert, D.E., Peeters, R., De Cock, P., Lagae, L., Sunaert, S., 2009. Construction of a stereotaxic DTI atlas with full diffusion tensor information for studying white matter maturation from childhood to adolescence using tractography-based segmentations. *Hum. Brain Mapp.* (NA–NA).
- Wang, F., Sun, Z., Cui, L., Du, X., Wang, X., Zhang, H., Cong, Z., Hong, N., Zhang, D., 2004. Anterior cingulum abnormalities in male patients with schizophrenia determined through diffusion tensor imaging. *Am. J. Psychiatry* 161, 573–575.
- Weinstein, M., Ben-Sira, L., Levy, Y., Zachor, D.A., Itzhak, E.B., Artzi, M., Tarrasch, R., Eksteine, P.M., Hendler, T., Bashat, D.B., 2010. Abnormal white matter integrity in young children with autism. *Hum. Brain Mapp.* 32, 534–543.
- Westerhausen, R., Huster, R.J., Kreuder, F., Wittling, W., Schweiger, E., 2007. Corticospinal tract asymmetries at the level of the internal capsule: is there an association with handedness? *Neuroimage* 37, 379–386.
- Westlye, L.T., Walhovd, K.B., Dale, A.M., Bjørnerud, A., Due-Tønnessen, P., Engvig, A., Grydeland, H., Tamnes, C.K., Ostby, Y., Fjell, A.M., 2010. Life-span changes of the human brain white matter: diffusion tensor imaging (DTI) and volumetry. *Cereb. Cortex* 20, 2055–2068.
- Wilde, E.A., McCauley, S.R., Chu, Z., Hunter, J.V., Bigler, E.D., Yallampalli, R., Wang, Z.J., Hanten, G., Li, X., Ramos, M.A., Sabir, S.H., Vasquez, A.C., Menefee, D., Levin, H.S., 2009. Diffusion tensor imaging of hemispheric asymmetries in the developing brain. *J. Clin. Exp. Neuropsychol.* 31, 205–218.
- Wolff, J.J., Gu, H., Gerig, G., Elison, J.T., Styner, M., Goutard, S., Botteron, K.N., Dager, S.R., Dawson, G., Estes, A.M., Evans, A.C., Hazlett, H.C., Kostopoulos, P., McKinstry, R.C., Paterson, S.J., Schultz, R.T., Zwaigenbaum, L., Piven, J., Network, I.B.I.S., 2012. Differences in white matter fiber tract development present from 6 to 24 months in infants with autism. *Am. J. Psychiatry* 169, 589–600.
- Wrase, J., Klein, S., Gruesser, S.M., Hermann, D., Flor, H., Mann, K., Braus, D.F., Heinz, A., 2003. Gender differences in the processing of standardized emotional visual stimuli in humans: a functional magnetic resonance imaging study. *Neurosci. Lett.* 348, 41–45.
- Yap, P.-T., Fan, Y., Chen, Y., Gilmore, J.H., Lin, W., Shen, D., 2011. Development trends of white matter connectivity in the first years of life. *PLoS One* 6, e24678.
- Yeatman, J.D., Dougherty, R.F., Rykhlevskaia, E., Sherbondy, A.J., Deutsch, G.K., Wandell, B.A., Ben-Shachar, M., 2011. Anatomical properties of the arcuate fasciculus predict phonological and reading skills in children. *J. Cogn. Neurosci.* 23, 3304–3317.
- Yeatman, J.D., Dougherty, R.F., Ben-Shachar, M., Wandell, B.A., 2012a. Development of white matter and reading skills. *Proc. Natl. Acad. Sci. U. S. A.* 109, E3045–E3053.
- Yeatman, J.D., Dougherty, R.F., Myall, N.J., Wandell, B.A., Feldman, H.M., 2012b. Tract profiles of white matter properties: automating fiber-tract quantification. *PLoS One* 7, e49790.
- Yücel, M., Stuart, G.W., Maruff, P., Velakoulis, D., Crowe, S.F., Savage, G., Pantelis, C., 2001. Hemispheric and gender-related differences in the gross morphology of the anterior cingulate/paracingulate cortex in normal volunteers: an MRI morphometric study. *Cereb. Cortex* 11, 17–25.
- Yücel, M., Wood, S.J., Phillips, L.J., Stuart, G.W., Smith, D.J., Yung, A., Velakoulis, D., McGorry, P.D., Pantelis, C., 2003. Morphology of the anterior cingulate cortex in young men at ultra-high risk of developing a psychotic illness. *Br. J. Psychiatry* 182, 518–524.
- Zhang, J., Jones, M., DeBoy, C.A., Reich, D.S., Farrell, J.A.D., Hoffman, P.N., Griffin, J.W., Sheikh, K.A., Miller, M.J., Mori, S., Calabresi, P.A., 2009. Diffusion tensor magnetic resonance imaging of Wallerian degeneration in rat spinal cord after dorsal root axotomy. *J. Neurosci.* 29, 3160–3171.